Lab on a Chip

Cite this: *Lab Chip*, 2011, **11**, 4057

www.rsc.org/loc

PAPER

Millifluidic droplet analyser for microbiology†

Larysa Baraban,*[a] Fabien Bertholle,[a] Merijn L. M. Salverda,[b] Nicolas Bremond,*[a] Pascal Panizza,[c] Jean Baudry,[a] J. Arjan G. M. de Visser[b] and Jérôme Bibette[a]

Received 22nd June 2011, Accepted 8th September 2011
DOI: 10.1039/c1lc20545e

We present a novel millifluidic droplet analyser (MDA) for precisely monitoring the dynamics of microbial populations over multiple generations in numerous ($\geq 10^3$) aqueous emulsion droplets ($\sim$100 nL). As a first application, we measure the growth rate of a bacterial strain and determine the minimal inhibitory concentration (MIC) for the antibiotic cefotaxime by incubating bacteria in a fine gradient of antibiotic concentrations. The detection of cell activity is based on the automated detection of an epifluorescent signal that allows the monitoring of microbial populations up to a size of $\sim 10^6$ cells. We believe that this device is helpful for the study of population dynamic consequences of microbe-environment interactions and of individual cell differences. Moreover, the fluidic machine may improve clinical tests, as it simplifies, automates and miniaturizes the screening of numerous microbial populations that grow and evolve in compartments with a finely tuned composition.

Introduction

Controlled operations of liquids at the micro scale are now surpassing the standard chemical and biological assays in laboratories. The various kinds of chemical or biological tests that are conventionally performed in millilitre and microlitre volumes (using test-tubes and microtitre plates) are now available in nanolitre or picolitre droplets.[1–8] Droplet-based fluidics is nowadays a high-performance technological upgrade of the well-known compartmentalization concept,[9,10] which has been used for directed evolution[11] and genome sequencing applications.[12] A key feature of this approach is that reactants and products are localized, thanks to the confinement, and that it leads to high product concentrations owing to small volumes. Moreover, for biological applications, phenotype and genotype are linked.

Encapsulation of microbial populations into droplets and the monitoring of their behavior is of great interest for both fundamental microbiology[13–16] and clinical tests.[17] In particular the experiments with single cells[4,5] are likely to be helpful in studies of the genetic and phenotypic variability of microorganisms.[18–21] On the other hand, use of the droplet-based concept for clinical assays can boost them to a new level in terms of precision and time efficiency. For instance, it can simplify the determination of resistance of bacterial isolates to antimicrobial agents.[22–25] This involves the determination of the minimal inhibitory concentration (MIC) of an antibiotic, which is conventionally performed either in microtitre plates, by using a serial 2-fold dilution method,[23] or by using antibiotic discs.[26] The MIC is then determined by a visual check of the growth/no-growth boundary between neighboring cultures, giving a binary yes/no response. Recently, Boedicker *et al.* demonstrated the possibility to perform antibiogram assays in droplets on a chip.[17]

Here, we present a novel *millifluidic droplet analyser* (MDA) that is designed to perform a variety of precise clinical and microbiological assays of microbial populations of sizes up to $\sim 10^6$ in more than 10^3 replicate droplets. The device represents a scale-up from the microfluidic approach, operating with larger droplets, but maintains the fundamental principles of fluid control and high throughput. A similar concept was also used earlier for the cultivation of monoclonal cell populations.[8,27] The MDA provides automation, increased precision and high performance, compared to classical techniques for microbiological analysis. In its present state, the fluidic machine performances are roughly similar to fully-automated microplate readers, but its lower cost offers an attractive and alternative tool. The MDA is capable of (i) pharmacodynamic assays in droplets *via* a fine tuning of each droplet composition (*e.g.*, MIC tests); (ii) creating a gradient of initial population sizes, ranging from 10^0–10^5 cells/drop; (iii) monitoring of microbial growth over many generations (including the detection of possible cooperation during growth in the presence of antibiotics[13,28,29]). Moreover, a straightforward implementation of a droplet sorter can be realized in order to select specific colonies from the droplet train.

[a]*UPMC Univ. Paris 06, CNRS UMR 7195, ESPCI ParisTech, 10 rue Vauquelin, 75231 Paris, France. E-mail: larysa.baraban@espci.fr; Fax: +33(0)140795245; Tel: +33(0)140795234*
[b]*Laboratory of Genetics, Wageningen University, 6708PB Wageningen, The Netherlands*
[c]*IPR, UMR CNRS 6251, Campus Beaulieu, Université Rennes 1, 35042 Rennes, France*
† Electronic supplementary information (ESI) available. See DOI: 10.1039/c1lc20545e

Materials and methods

Concept

In contrast to microfluidic approaches working with picolitre reservoirs, droplets in millifluidic systems have volumes of around 100 nL.[8,27,30,31] Therefore, the technology is adapted to much larger total volumes by switching from microchannels used in PDMS chips to commercially available transparent fluorinated ethylene propylene (FEP) tubes with an inner diameter (ID) of 0.5 mm (see Fig. 1S, ESI†).

The use of the FEP tubing ensures a good wettability of the continuous phase, and prohibits droplets sticking on the wall during operation of the device. A key feature of this technology is the assembly of various modules with a specific function (droplet formation, droplet fusion, droplet fragmentation, *etc.*) like in microfluidic systems,[32] but with fluidic components used in the field of chromatography (Upchurch Scientific and VICI Valco Instruments) and electric valve actuators (LFR and LFV-Series micro inert valves, LEE Company) for controlling fluid flow direction (see Fig. 1S, ESI†). For instance, the cross-junctions of the device (*Cross A*, *Cross B* in Fig. 1), used for droplet formation, are commercially available tools (P-634, Upchurch Scientific). The FEP tubes are connected to the cross-junctions *via* flangeless fittings with standard $^1/_4$–28 thread (flangeless nut and ferrule: P-245X and P-200X respectively, Upchurch Scientific). Other interconnections in the circuit, *i.e.* syringes, electric valves, and wastes, are realized utilizing the same fittings.

The MDA operates more than 10^3 separate water-in-oil droplets that act as "mini incubators" for the encapsulated living cells. In the present configuration, the fluidic machine is adapted to study the growth of microorganisms *via* the detection of a fluorescent signal. Therefore, we use a strain containing a fluorescent protein reporter that allows the measurement of population size in each drop.[20] As was mentioned above, droplets are produced in cross-junction geometry and form a one-dimensional train where each droplet represents an element of a numeric sequence. Because the size of the droplets slightly exceeds the inner diameter of the FEP tube (length of the droplet ~0.75 mm *versus* tube ID 0.5 mm), their order is preserved during the experiment. The linear geometry therefore leads to a self-labelling of each aqueous reservoir that contains living cells. Identification of the droplets allows us: 1) to form a "database" for each bacterial population in the drop train; 2) to accumulate the growth data for each population; 3) to potentially access a population of interest by sorting and isolating specific droplets at the end of the experiment.

A sketch of the MDA is presented in Fig. 1. It consists of two basic interconnected modules: a drop maker and a detector.

Drop maker

The drop maker module is aimed to form a large number of isolated aqueous droplets containing microorganisms in predefined microenvironments. It provides a control over the initial population size N_0 (inoculum) and environmental conditions (*e.g.* nutrients, antibiotics, drugs, *etc.*) of each drop. The procedure of droplet formation is as follows (see Fig. 1a): Solutions of bacteria, nutrients and antibiotics are prepared and stored into three separate syringes (*Syringe-Antb.*, *Syringe-LB*, *and Syringe-Bact.*). These solutions are injected by independent high-precision syringe pumps (neMESYS, Cetoni) and are then mixed at a cross junction (*Cross A*). The train of uniform droplets containing bacteria and dispersed in hydrofluoroether oil (HFE-7500, 3M) (*Syringe-Oil*) is formed at a cross-junction

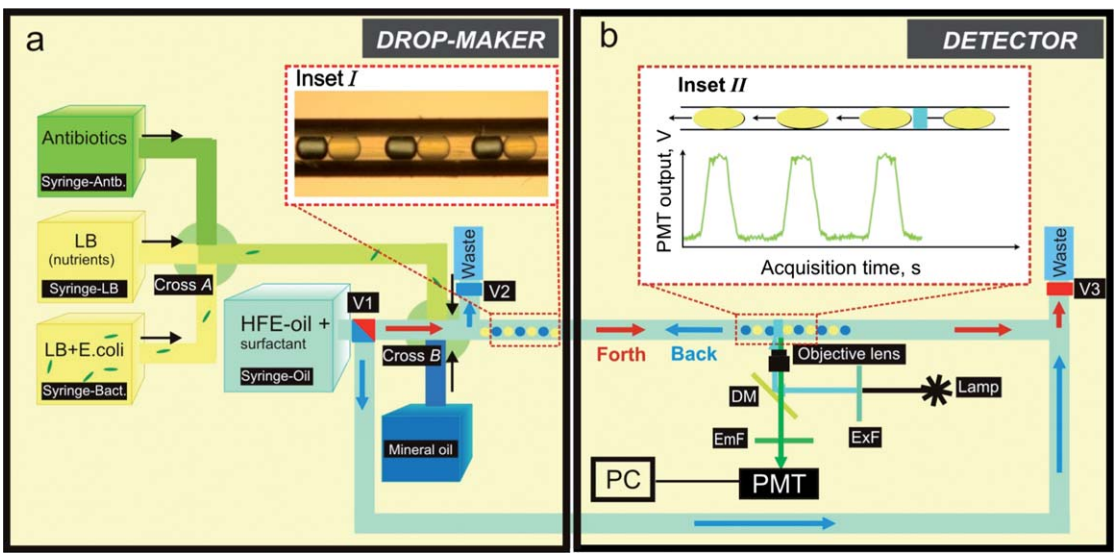

Fig. 1 Schematic description of the millifluidic device. (**a**) *Drop-maker*: this module is used for encapsulating the bacteria into droplets with a tuneable culture medium composition. Components like antibiotics, nutrients and bacteria are independently injected and then mixed at cross-junction *Cross A*. Water-in-oil droplets are formed at *Cross B* by using HFE oil as the continuous phase. Mineral oil droplets are also formed and act as spacers between aqueous reservoirs. A droplet train with alternating droplets of mineral oil and culture medium with bacteria is displayed in Inset *I*. (**b**) *Detector*: this module measures the growth of the bacterial populations over time. The module consists of a *back-and-forth* circuit, equipped with electric valves (V1, V2 and V3) and a fluorescent detection system. The droplet train is pushed toward the detector by injecting HFE oil into the circuit (Syringe-Oil). As the droplet passes the detector, the fluorescent signal emitted from each droplet is recorded (Inset *II*).

(*Cross B*, Fig. 1S(a), ESI†). To avoid the coalescence of the neighboring reservoirs and the wetting on the tube's wall, 0.006% of highly biocompatible tri-block copolymer surfactant is added to the HFE phase. In order to spatially separate the neighboring bacterial populations, spacer droplets of mineral oil (M5904, Sigma Aldrich) are injected at *Cross B* between the aqueous drops (see inset *I* in Fig. 1a). This step is crucial for the performance of the whole machine because the high density of the droplets causes the appearance of so-called "traffic jams" in the tubes[33] and may lead to the possible overlapping of the fluorescent signals from the neighboring bacterial populations during detection. Therefore, mineral oil and aqueous solution with bacteria appear as a one-dimensional train of about 2000 droplets in alternating order. The frequency of droplet formation is maintained constant at $f = 13$ Hz, using the following flow rates $Q_{HFE} = 6$ mL h^{-1}, $Q_{MO} = 6$ mL h^{-1}, $Q_W = 4$ mL h^{-1} for the injection of HFE oil, mineral oil and bacterial suspension, respectively. The flow rate Q_W represents the sum of the flow rates for injection of bacteria Q_B, pure medium Q_{LB}, and antibiotics Q_{Antb}. When the required number of droplets has been produced, the formation process is stopped. About 200–300 droplets at both extremities of the train are removed (using the electric valves V2, V3 to control the flow, Fig. 1a–b) in order to make a buffer volume free of emulsion drops. Finally, two plugs of mineral oil are injected at both ends of the droplet train in order to avoid any boundary effect like a higher oxygen transfer from the HFE oil to the drops.

Screening assays. Here, we demonstrate the MDA's capabilities to perform precise measurements of bacterial resistance to antibiotics, which are of interest for microbiological and clinical applications. The fine-tuning of the microenvironments for bacterial growth is provided by a gradual change of antibiotic concentrations from droplet to droplet, while the initial bacterial population size N_0 is kept constant. In order to maintain the droplet volume constant during the formation of the antibiotic gradient, the total flow rate of the droplet components has to remain the same ($Q_W = 4$ mL h^{-1}). This is achieved by independently injecting three aqueous solutions that finally compose the droplets: medium with bacteria Q_B, pure medium Q_{LB}, and medium with antibiotics Q_{Antb}. The flow rate of the phase containing the bacteria is maintained constant during the formation of the entire train ($Q_{Bact} = 2$ mL h^{-1}). While the flow rate of the phase containing the antibiotics is decreasing, the injection of pure nutrient medium is simultaneously increasing at a complementary rate. Fluorescent markers (green fluorescent colloids having a diameter of 3 μm) are added to the antibiotic solution in order to evaluate the antibiotic concentration in each drop. The formation of an antibiotic gradient across a 10-fold dilution is reported in Fig. 2. The green curve in Fig. 2a shows a one-step change of the flow rate $Q_{Antb.}$ of the syringe from 1 mL h^{-1} to 0.1 mL h^{-1}. In turn, the red curve displays the simultaneous change of the flow rate Q_{LB} (nutrients) from 1 mL h^{-1} to 1.9 mL h^{-1}. Fig. 2b displays the resulting profile of fluorescent signal (shown in red color; the inset of the figure shows the signal from the antibiotic concentration as function of droplet number), reflecting a 10-fold decrease of antibiotic concentration along the train of droplets. The resulting gradient differs from a step-like profile due to inertia in the response of the fluidic circuit linked to elastic deformations of the solid walls (mainly the tube) and the syringe pump itself. As far as the value of the fluorescent signal is proportional to the amount of injected antibiotics, the concentration of the antibiotic in each droplet can be estimated. For the present example of 10-fold dilution, about 800 droplets compose the gradient (see inset in Fig. 2b). This method for obtaining a gradient can be applied to screen different ranges of antibiotic concentrations, but can also be extended to other applications, like the formation of a precise gradient of initial cell number or nutrient concentration along the droplet train.

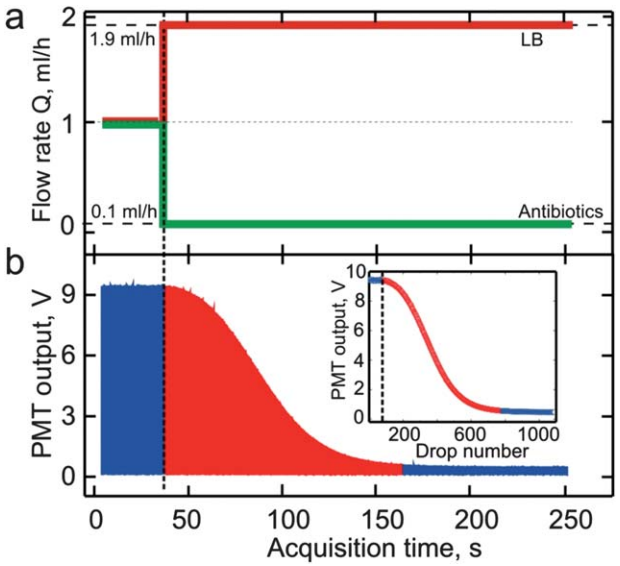

Fig. 2 Formation of a gradient of antibiotics. (**a**) Step-like change of the flow rates used to inject the antibiotics (shown in green) and LB medium (red). The resulting concentration of antibiotics is quantified by incorporating fluorescent colloidal particles in the antibiotic solution. (**b**) Concentration of antibiotics as a function of time after the flow rate switch shown in (a). Inset: Relation between fluorescent signal (linked to the concentration of antibiotics) and droplet number. Note that the noise of the fluorescent signal readout is estimated as 0.1 V (data not shown).

Detector

Changes in cell number are deduced *via* the measurement of fluorescence inside each droplet. The detection module, shown in Fig. 1b, consists of a fluorescence detector and a so-called "*back-and-forth*" circuit. The detector in the MDA is equipped with a photomultiplier tube (PMT). The excitation light is provided by a mercury lamp which is filtered by an excitation filter (ExF) (wave lengths around ~490 nm) and focused by a 20×-objective on the transparent FEP tube containing the train of droplets. The tube center is positioned at the focal plane of the objective lens resulting in a light spot diameter close to 1 mm. The emitted fluorescent light passes through a dichroic mirror (DM) and an emission filter (EmF, wavelengths around ~525 nm) and is finally collected by the photocathode of the PMT. Because the detection point is fixed, we initiate the motion of the droplet train towards the detector by injecting the continuous phase at a given flow rate. The droplets are therefore sampled one by one at a fixed frequency. An example of the fluorescent signal that is emitted from the bacteria entrapped in the droplets is reported in

Fig. 1b (Inset *II*). The growth history of each bacterial population can be followed by repeating the scan of the train during several hours. This is realized by using a back-and-forth strategy. The fluidic circuit consists of a closed loop containing the droplets, and a 3-way electric valve (V1) to control the flow direction. When the scan of the full train of droplets in the "*forth*" direction is completed, valve V1 is automatically switched, initiating the reverse motion of the droplets in the circuit and providing a subsequent "*back*" run of drop sampling. The sampling frequency is controlled *via* the continuous flow rate Q_{HFE}. In the present application, Q_{HFE} is equal to 4 mL h^{-1} and results in a sampling frequency of about 4 Hz. Each droplet is passing through the detecting spot around 8 times per hour. Therefore, the number of cells contained in each droplet is measured every 7 to 8 min.

After the first scan, each droplet in the train acquires a serial number that identifies the droplet for subsequent measurements. Information about changes of the fluorescent signal of the bacterial populations is gradually accumulated *via* performing multiple runs during 10 to 12 h. Acquisition of the analogical signal from the PMT and the control of the electric valves are performed using data acquisition hardware and a specially developed Lab View program.

Bacteria

Capabilities of the device are demonstrated using *Escherichia coli* strain MC4100-YFP, containing the constitutively-expressed yellow (*yfp*) allele of GFP inserted in the *galK* locus in the bacterial chromosome.[20,21] The relationship between the fluorescent signal and the number of cells within the droplets is reported in Fig. 3. The calibration is obtained by using solutions with known concentrations of bacteria that are deduced from optical density measurements with a UV spectrometer. These solutions are immediately used to form droplets which are then rapidly measured by using the MDA machine. Fig. 3 shows that the fluorescent signal depends linearly on cell number. Moreover, we determine that the detection limit N^* of the device, which is the minimal population size in droplets that can be detected, is close to 2000 cells/droplet. The protocol of the cell culture and manipulation for growth experiments is described in more details in the supplementary information.

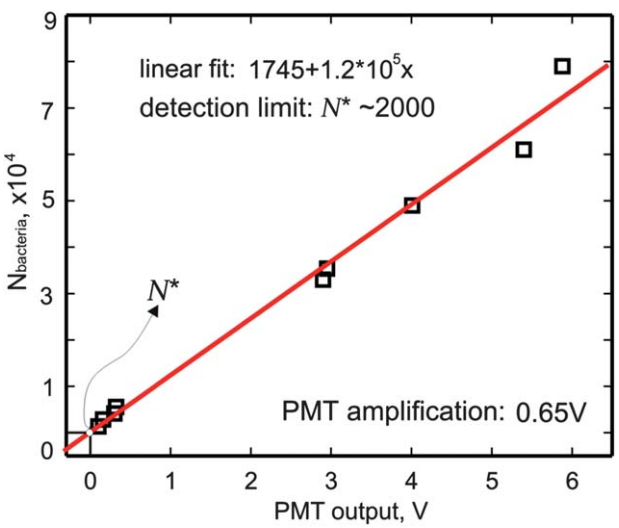

Fig. 3 Calibration of the number of bacteria inside the droplets as a function of their fluorescent signal. The detection limit N^* of the detection module is close to 2000 cells per droplet.

The dynamics of growth and the final population size are influenced by the amount of nutrients, the concentration of antibiotics and by the external conditions (*e.g.* temperature, aeration).[34,35] Here, all the experiments are performed at a fixed temperature of 37 °C by setting the fluidic machine in a temperature-controlled chamber. The growth conditions for the bacteria in the droplets are different from those prevailing in standard test tubes or microtitre plates. First, the absence of hard-surface walls in the droplets and the hydrodynamic mixing of injected components reduce the probability of filamentous growth and prevent bio-film formation on a wall, which affect the resistance of bacterial populations to antibiotics.[24] Second, the access of cells to oxygen inside droplets is probably limited due to the encapsulation of the droplets inside a tube and the presence of mineral oil slugs at both ends of the droplet train. Although *E. coli* is a facultative anaerobic organism, aeration is known as one of the factors to affect the average doubling time τ of the population and the final biomass produced.[35]

Results and discussions

Growth kinetics

As a first test of the fluidic machine, we measure the growth of more than 1000 populations from an initial concentration, N_0, of 1000 cells/droplet in LB medium. The growth curves reported in Fig. 4a show the conventional lag, exponential and stationary phases of bacterial growth.[34] In our experiments, an apparent lag phase reflects the time needed for the bacterial populations to reach the size equivalent to detection limit N^*; thus, we assume that the time contribution needed for physiological adaptation to the growth conditions in the droplet is negligible, because cells were taken from exponentially growing cultures using the same growth medium (see ESI†). The increase of the bacterial population size during exponential phase over time is described by $N(t) \sim N_0\ 2^{t/\tau}$, where τ is the average doubling time of the population.[34] As soon as the available nutrients that enable growth are exhausted, the cells enter into the stationary phase, eventually followed by a death phase. We note that the transition to stationary phase occurs at nearly the same time (*i.e.* ~350 min) for all populations. In addition, the growth curves reach a plateau that is characterized by a narrow distribution of the final biomass $N_{final} \approx 2.7 \times 10^5$ cells/droplet, with a coefficient of variation of $N_{final} \approx 9000$ cells/droplet. Fig. 4b displays the distribution of estimated doubling times τ, calculated for each population in the train. The average doubling time of bacterial droplet populations is 33.8 min with a standard deviation of 0.3 min, which is comparable to the values, measured in standard culturing methods.[36] The high reproducibility of growth curves and small variance of τ demonstrate that the growth conditions are homogeneous across droplets and the fluorescent signal is measured with high accuracy.

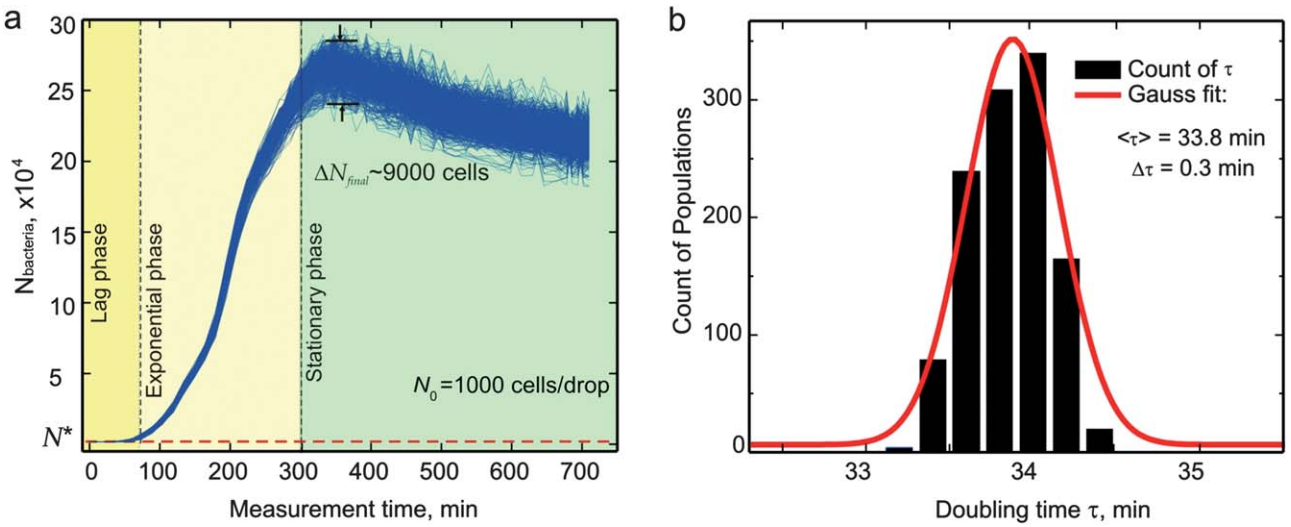

Fig. 4 Growth of the bacteria in droplets. (**a**) Growth curves of the bacteria in droplets, measured for 1 193 populations. Initial population size of *E. coli* is $N_0 = 1000$ cells/droplet. The growth dynamics consist of a lag phase, an exponential phase and a stationary phase, which are indicated in different colors. N^* is marked with a red dashed line as the lowest population size of bacteria that can be detected by the system. (**b**) Distribution of the doubling time τ among the 1 193 bacterial populations.

MIC assays

Here, we demonstrate the capability of the MDA to determine the MIC of this *E. coli* strain for the antibiotic cefotaxime (CTX). The MIC of a bacterial population is one of the widely used pharmacodynamic parameters that characterizes resistance levels and determines the antibiotic dose to be administered. In standard MIC assays (96-wells microplate protocol), a fixed inoculum of bacteria is injected into media with different concentrations of antibiotic. The MIC is defined as the lowest concentration of antibiotic applied that inhibits visible growth of the bacterial population. A step-wise change of antibiotic concentrations (usually 2-fold, *i.e.* 100% concentration difference of adjacent concentrations) determines the precision of the MIC estimate. Here, we determine the MIC with a precision of about two orders of magnitude higher (*i.e.* ~1% difference in adjacent antibiotic concentrations); the step-size in our device is expected to be around $\Delta C \sim (C_{MAX} - C_{MIN})/N^g{}_D$, where C_{MAX} and C_{MIN} define the range of antibiotic concentrations and $N^g{}_D$ is the number of droplets (steps) composing the gradient. This statement is displayed in Fig. 2S (ESI†), where the cefotaxime concentration is calibrated against drop number for MDA and number of dilution steps for the microplate. One can see that the MDA performs $N^g{}_D \approx 800$ steps to cover the concentration range of 0.0015–0.03 μg CTX mL^{-1}, while the microplate technique offers only $N^g = 6$.

The MIC assay for CTX using an $N_0 = 10$ cells/droplet are shown in Fig. 5. In order to find the MIC, a gradient of CTX concentrations in the range of 0.0015–0.03 μg (CTX) mL^{-1} was formed in a train of $N_D = 1320$ droplets. In contrast to the growth curve measurements where all populations face the same conditions, now bacteria in the droplets encounter gradually increasing antibiotic stress. Fig. 5a and 5b show the profile of fluorescent signal for all droplets at the beginning of the experiment ($T = 0$ min) and after 7 h ($T = 400$ min), respectively. The plots can be visually divided in two parts, shown in blue and red respectively. The boundary between these two parts coincides with the MIC level. On the right hand side (blue), antibiotic concentrations were sufficiently low to allow bacterial growth. In contrast, the signal remains unchanged in droplets on the left hand side (red), where the concentration of CTX is equal to or higher than the MIC. Bacterial growth is partially suppressed in the so-called sub-MIC region, and stays weakly affected at lower CTX concentrations. The dynamics of the microbial populations affected by the antibiotics are presented in Fig. 5c. The figure displays a color-coded series of growth curves of the bacteria in the droplets with a gradient of CTX concentrations. We define MIC as the concentration of antibiotic inside the first droplet that does not reveal positive growth above the detection limit N^* (red dashed line in Fig. 5c). In that case, the MIC is determined at 0.009 μg CTX mL^{-1}. In order to check the reproducibility of the MIC determination, we performed three assays for $N_0 = 10$ cells/droplet using the MDA machine. Obtained values of MIC reveal weak deviations (<5%) from the reported value 0.009 μg CTX mL^{-1}. For comparison, the CTX MIC for this strain measured in a standard MIC assay in 100 μL cultures in a microtitre plate is slightly higher, 0.03 μg mL^{-1}. The precision of this estimate is limited by the methodology: namely, 2-fold serial dilution determines the step-size and accuracy of the measurement (see Fig. 2S, ESI†). The discrepancy between droplets and microplate methods is probably caused by differences in growth conditions (*e.g.* inoculum size) and different criteria for the MIC determination (visual check *versus* fluorescent detection).

The detailed graph provides a comprehensive characterization of the population dynamic behavior of the bacteria in the antibiotic gradient. For instance, one can observe that variation in CTX concentration hardly influences the growth rate. In contrast, the final population size at sub-MIC concentrations is strongly affected. A similar tendency has been previously shown,[37] where the authors hypothesized that in the presence of antibiotics bacteria consume more glucose to maintain the same microbial population size. This maintenance energy increases with antibiotic concentration.

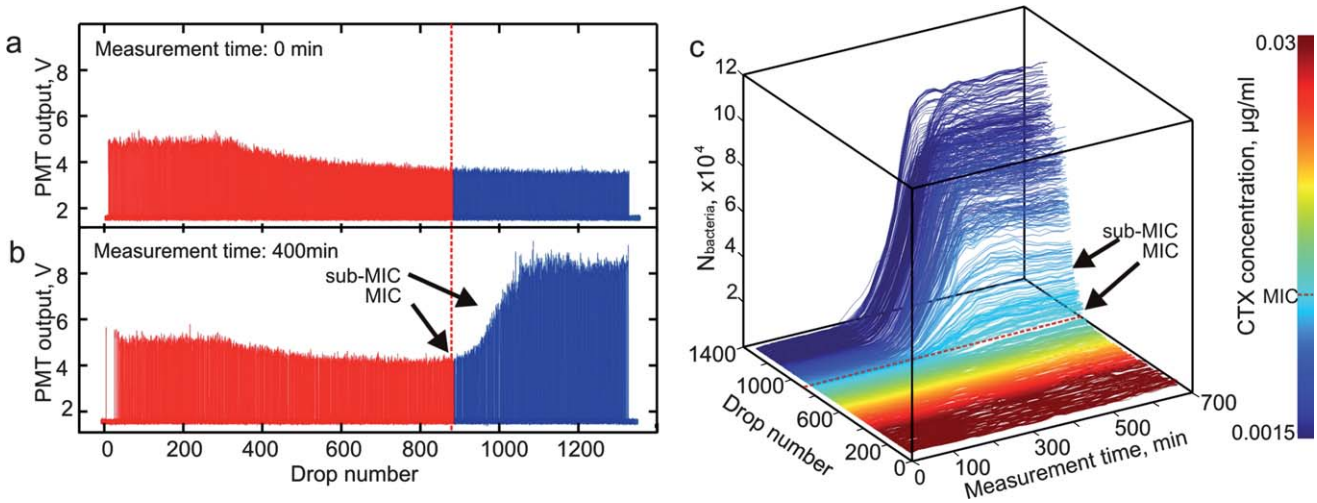

Fig. 5 Determination of the MIC for inoculum size $N_0 = 10$ cells/droplet. (**a**) Fluorescent signal measured in each droplet of the train at the beginning of the experiment. The decrease of the fluorescent signal reflects the gradient of antibiotics that is injected into the droplets. (**b**) Intensity of the fluorescence as a function of droplet number after 400 min. (**c**) Growth curves of the bacterial populations, grown in the gradient of CTX concentrations ranging from 0.03 to 0.0015 μg mL^{-1}. The color mapping corresponds to a droplet number that is linked to a concentration of CTX.

Conclusion

Here, a novel millifluidic droplet analyser (MDA), capable of monitoring the history of a large number of microbial cultures that grow in water-in-oil emulsion droplets, is presented. The automated fluidic machine can manipulate and monitor each of more than 1000 microbial populations inside aqueous reservoirs of ~100 nL. The linear geometry of the system provides a self-labelling of each droplet, and therefore of each cell population. The experimental approach allows one to perform quantitative statistical analyses of cell population growth, as well as a detailed screening of the effect of medium composition on growth.

We demonstrate the capabilities of the automated fluidic machine by quantifying the distribution of the doubling time of monoclonal populations of *E. coli* and by determining the resistance level (MIC) of bacteria to an antibiotic with unprecedented precision. We believe that the new MDA can become useful in academic laboratories or in industries as an efficient tool with a relatively low cost for screening the survival and growth kinetics of microorganisms under various culture conditions. Moreover, we are currently developing detection systems based on light scattering to extend the existing capabilities of the machine to microbial strains without fluorescent markers, as well as detection systems for the simultaneous monitoring of multiple fluorescent signals to quantify microbial fitness during direct competition. Finally, we are implementing a droplet sorter for the selection of specific populations based on their growth dynamics. This module may be suitable for drug screening applications or for transferring populations of microorganisms in serial-dilution evolution experiments.

Notes and references

1 A. J. DeMello, *Nature*, 2006, **442**, 394.
2 J. El-Ali, P. K. Sorger and K. F. Jensen, *Nature*, 2006, **442**, 403.
3 M. Joanicot and A. Ajdari, *Science*, 2005, **309**, 513.
4 J. Clausell-Tormos, *et al.*, *Chem. Biol.*, 2008, **15**, 427.
5 S. Koester, *et al.*, *Lab Chip*, 2008, **8**, 1110.
6 C. Holtze, *et al.*, *Lab Chip*, 2008, **8**, 1632.
7 A. B. Theberge, *et al.*, *Angew. Chem., Int. Ed*, 2010, **49**, 5846.
8 K. Martin, T. Henkel, V. Baier, A. Grodrian, T. Schon, M. Roth, J. M. Koehler and J. Metze, *Lab Chip*, 2003, **3**, 202.
9 G. J. V. Nossal and J. Lederberg, *Nature*, 1958, **181**, 1419.
10 B. Rotman, *Proc. Natl. Acad. Sci. U. S. A.*, 1961, **47**, 1981.
11 D. S. Tawfik and A. D. Griffiths, *Nat. Biotechnol.*, 1998, **16**, 652.
12 M. Margulies, *et al.*, *Nature*, 2005, **437**, 376.
13 J. Q. Boedicker, M. E. Vincent and R. F. Ismagilov, *Angew. Chem., Int. Ed.*, 2009, **48**, 5908.
14 A. Groisman, *et al.*, *Nat. Methods*, 2005, **2**, 685.
15 F. K. Balagaddé, L. You, C. L. Hansen, F. H. Arnold and S. R. Quake, *Science*, 2005, **309**, 137.
16 M. Chabert and J.-L. Viovy, *Proc. Natl. Acad. Sci. U. S. A.*, 2008, **105**, 3191.
17 J. Q. Boedicker, *et al.*, *Lab Chip*, 2008, **8**, 1265.
18 J. M. Raser and E. K. O'Shea, *Science*, 2005, **309**, 2010.
19 A. Raj and A. Van Oudenaarden, *Cell*, 2008, **135**, 216.
20 M. Hegreness, N. Shoresh, D. Hartl and R. Kishony, *Science*, 2006, **311**, 1615.
21 M. B. Elowitz, A. J. Levine, E. D. Siggia and P. S. Swain, *Science*, 2002, **297**, 1183.
22 B. Vogelman and W. A. Craig, *J Pediatr.*, 1998, **108**(5(2)), 835.
23 R. J. W. Lambert, *J. Appl. Microbiol.*, 2000, **89**, 275.
24 P. S. Stewart and J. W. Costerton, *Lancet*, 2001, **358**, 135.
25 H. Steels, S. A. James, I. N. Roberts and M. Stratford, *Yeast*, 2000, **16**, 1173.
26 T. D. Wilkins, L. V. Holdeman, I. J. Abramson and W. E. C. Moore, *Antimicrob Agents Chemother.*, 1972, **1**(6), 451.
27 A. Funfak, A. Brösing, M. Brand and J. M. Koeler, *Lab Chip*, 2007, **7**, 1132.
28 H. H. Lee, M. N. Molla, C. R. Cantor and J. J. Collins, *Nature*, 2010, **467**, 82.
29 N. Q. Balaban, J. Merrin, R. Chait, L. Kowalik and S. Leibler, *Science*, 2004, **305**, 1622.
30 W. Engl, R. Backov and P. Panizza, *Curr. Opin. Colloid Interface Sci.*, 2008, **13**, 206.
31 V. Trivedi, *et al.*, *Lab Chip*, 2010, **10**, 2433.
32 B. Kintses, L. D. van Vliet, S. R. A. Devenish and F. Hollfelder, *Curr. Opin. Chem. Biol.*, 2010, **14**, 548.
33 N. Champagne, R. Vasseur, A. Montourcy and D. Bartolo, *Phys. Rev. Lett.*, 2010, **105**, 044502.
34 J. Monod, *Annu. Rev. Microbiol.*, 1949, **3**, 371.
35 M. A. Juergensmeyer, E. S. Nelson and E. A. Juergensmeyer, *Lett. Appl. Microbiol.*, 2007, **45**, 179.
36 G. Sezonov, D. Joseleau-Petit and R. D'Ari, *J. Bacteriol.*, 2007, **189**, 8746.
37 J. R. Lobry, G. Carret and J. P. Flandrois, *J. Antimicrob. Chemother.*, 1992, **29**, 121.